

Simultaneous Determination of Hydroquinone and Catechol using Carbon Glass Electrode Modified with Graphene Quantum Dots

Jing Tang^{1*}, Xiaoqing Ma¹, Jing Liu¹, Shengbiao Zheng¹, Jianfei Wang^{2*}

¹College of Chemistry and Material Engineering, Anhui Science and Technology University, 233100, Fengyang, Anhui Province, China

²College of Resource and Environment, Anhui Science and Technology University, 233100, Fengyang, Anhui Province, China

*E-mail: zhengtang102@163.com (Tang Jing), wangjf@ahstu.edu.cn (Wang Jianfei)

Received: 6 July 2018 / Accepted: 29 August 2018 / Published: 1 October 2018

In this study, an electrochemical sensor for the simultaneous detection of hydroquinone (HQ) and catechol (CC) was fabricated on glassy carbon electrode (GCE) modified with graphene quantum dots (GQDs). The prepared GQDs were characterized by transmission electron microscope and fourier transform infrared spectroscopy. The GQDs/GCE, which prepared by electrodeposition method, and characterized by electrochemical impedance spectra, exhibited excellent electrochemical catalysis and conductive properties for HQ and CC. Owing to the high electroactive surface area, good electrocatalytic activity and low charge transfer resistance of GQDs, HQ and CC can be easily measured simultaneously for the large separation of oxidation peak potentials (113 mV) and do not interfere with each other. Under the optimal experimental condition, the oxidation peak currents were linear to HQ/CC in the range from 0.5 μM to 100 μM with the same low detection limits of 0.08 μM (S/N=3). Simultaneous determination of HQ and CC with such electrode was conducted in river water samples with reliable recovery between 97.90% and 103.9%.

Keywords: graphene quantum dots; hydroquinone; catechol; simultaneous; modified electrode

1. INTRODUCTION

Hydroquinone (1, 4-dihydroxybenzene, HQ) and catechol (1, 2-dihydroxybenzene, CC), as two isomers of dihydroxybenzene, are often used in key industrial raw materials, synthetic intermediates and some chemicals, such as plastics, rubber, medicine and so on [1]. Even in a very low concentration of HQ and CC are extremely toxic to environment and humans. Because of difficult to degrade, they are the major problem and cause for the environment pollution [2, 3]. In addition, since HQ and CC have similar structures and properties, they usually coexist when they are synthesized and used. Therefore,

the development of an easy, facile, sensitive and accurate method for simultaneous determination of dihydroxybenzene isomers analysis is crucial [4-6]. Various methods have been developed by means of high-performance liquid chromatography (HPLC) [7], synchronous fluorescence [8], chemiluminescence [9, 10], spectrophotometry [11], capillary electrophoresis [12], electrochemical methods [13-15], and pH based-flow injection analysis [16]. Compared with other analytical methods, electrochemical methods have attracted a great deal of interest from researchers due to its unique high sensitivity and ease of operation, as well as its advantages of rapid detection and low instrument maintenance costs. However, a major problem is that the electrochemical oxidation of dihydroxybenzene isomers located at high overpotentials and their oxidation peaks are seriously overlapped using conventional electrodes. In recent years, some researchers have used novel materials modified on the surface of GCE to increase the separation of peaks potential of these two isomers and increase the redox current value [17, 18]. For example, Lu et al. [18] reported that the prepared MIL-101(Cr)-rGO to modify carbon paste electrode for the quantitatively detection of HQ and CC.

Among carbon materials, graphene quantum dots (GQDs) are graphene nanosheets with a three-dimensional scale of less than 100 nanometers, and they have also been studied recently for new types of carbon materials [19]. GQDs, which synthesized by a relatively simple synthetic method, exhibits the advantages of good conductivity and fast electron transfer, and can be well compatible with organisms and low in toxicity in cells [20, 21]. Furthermore, GQDs contain many functional groups, such as hydroxyl, carbonyl and carboxylic acid groups [22]. Some researchers have reported that GQDs has potential applications in the field of battery electrode materials and efficient catalysts [23-25]. Due to the excellent electronic properties and zero-dimensional spatial structure of GQDs, some researchers modified it as a modifying material to the electrode surface to improve the electrode performance [26-28]. Our group have used GQDs modified electrode to determine dopamine with high sensitivity [27]. Wang et al. used GQDs and silver nanoparticles modified GCE for simultaneous determination of guanine and adenine [28]. Therefore, GQDs have the potential to be used as excellent materials to modify electrodes for electrochemical platform. However, to our knowledge, there are no reports on employing GQDs as an electrode sensing material towards HQ and CC.

In this study, we have made full use of the advantages of GQDs, such as electron transport properties and electrocatalytic performance. The GQDs were electrodeposited onto the GCE surface as an electrochemical sensor for simultaneous determination of HQ and CC. The GQDs modified electrode exhibited high electrocatalytic activity towards HQ and CC with the separated oxidation peak potential of 113 mV. The prepared modified electrode revealed high sensitivity, reliability and reproducibility in the electrochemical measurement, achieving the detection limit down to 0.08 μM .

2. MATERIALS AND METHODS

2.1 Materials

HQ and CC were supplied by Aladdin (China) and were stored at 4 °C in dark. The stock solutions of 1.0×10^{-3} M HQ and 1.0×10^{-3} M CC was prepared in double distilled water. Citric acid (CA) and glucose were received from Sigma-Aldrich (USA). Phosphate buffer solution (PBS, 0.1 M) was prepared by mixing the stock solution of standard 0.1 M NaH_2PO_4 and 0.1 M Na_2HPO_4 solutions and adjusting

the pH with H_3PO_4 or NaOH . All chemicals are analytical grade without any further purification. The double distilled water (resistivity $> 18 \text{ M}\Omega \text{ cm}$) was used throughout the studies.

2.2 Apparatus

The electrochemical experiments (cyclic voltammetry and differential pulse voltammetry) were done on CHI660E electrochemical workstation (Shanghai ChenHua Instruments Corporation, China) with a three-electrode cell. A bare GCE or the GQDs modified GCE was used as a working electrode. The platinum wire electrode was employed as auxiliary electrode and reference electrode was a saturated calomel electrode (SCE). Electrochemical impedance spectroscopy (EIS) experiments were done on Princeton PARSTAT 4000 between 0.1 Hz and 10 kHz at 0.25 V. All the redox potentials of analytes were recorded versus the SCE at ambient temperature. The morphology and size of the synthesis GQDs was observed by transmission electron microscope (TEM) (JEM 2100, Tokyo, Japan) with an acceleration voltage of 200 kV. Fourier transform infrared spectroscopy (FT-IR) in the range of 4000–500 cm^{-1} was performed on a Thermo Fisher FT-IR spectrometer.

2.3 Synthesis of GQDs

The GQDs were prepared via the bottom-up pyrolysis method [29]. In brief, 2 g CA was placed in a 100 mL round bottom flask and then heated to 200 °C for 30 min in an oil bath. The color of the liquid changed from colorless to orange, implying the formation of GQDs. And then, this orange liquid was dissolved by dropwise addition of 10 $\text{mg}\cdot\text{mL}^{-1}$ NaOH solution with vigorous stirring until the pH of the solution up to 8.0. Lastly, the GQDs were dialyzed for 36 h with the dialysis bags (retained molecular weight: 3500 Da), and after vacuum freeze dry, the GQDs were stored at 4 °C in a refrigerator.

2.4 Electrode Preparation

Before the modification, the GCE were carefully polished to mirror-like with 0.05 mm alumina slurry, rinsed thoroughly with double distilled water and then treated with HNO_3 (1:1), ethanol, double distilled water in sequence. The surface of GCE was dried with nitrogen. Electrodeposition of GQDs at the surface of bare GCE was carried out by using cyclic voltammetric method in aqueous solution containing 2 $\text{mg}\cdot\text{mL}^{-1}$ GQDs solution in 0.1 M PBS of pH 7.0. The electrodeposition was achieved by the formation of a film that grew between -1.5 V to $+2.0 \text{ V}$ at the scan rate of 100 mV s^{-1} for 18 cycles. After this the electrode was rinsed thoroughly with double distilled water.

3. RESULTS AND DISCUSSION

3.1 Characterization of GQDs

Fig.1 shows the TEM image of GQDs. These spherical nanoparticles have a size between 3 nm and 18 nm, and the average sizes of the GQDs about 10 nm. As show in Fig. 2, FTIR can also be used to characterize the structural information of GQDs. The GQDs exhibited strong absorption of stretching

vibration of C=O at 1640 cm^{-1} , stretching vibration of C–H at 1355 cm^{-1} and C–OH at 1120 cm^{-1} , which indicated the GQDs may contain carboxyl. Furthermore, the GQDs showed absorption of stretching vibration O–H at 3444 cm^{-1} , indicating that GQDs contain hydroxyl groups [30]. These results further confirmed that the GQDs have been successfully prepared.

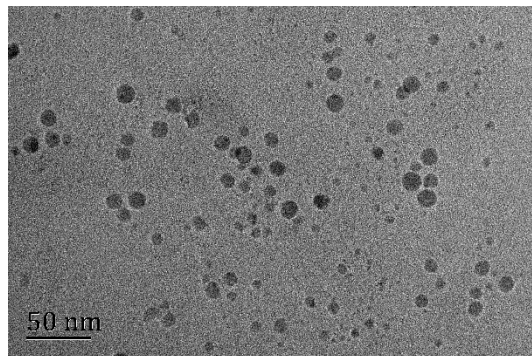


Figure 1. TEM image of GQDs [27]

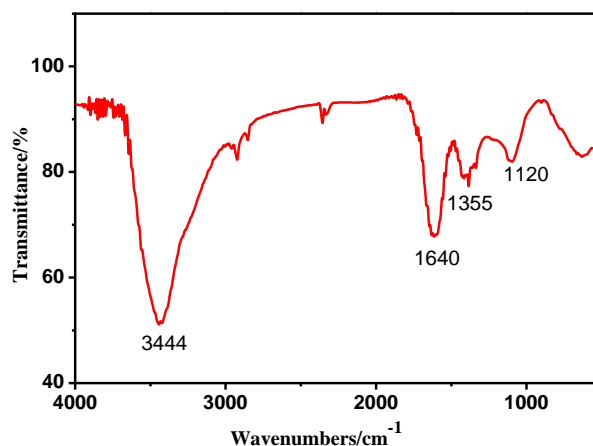


Figure 2. FTIR of GQDs

3.2 Electrochemical characterization of the GQDs/GCE

EIS is an effective method to probe the change of interface properties of electrode surface. The EIS of different electrodes measured with a frequency ranging from 0.1 to 100 kHz in 0.1 M KCl electrolyte solution including 5 mM $\text{Fe}(\text{CN})_6^{4-/3-}$. As shown in Fig. 3, the nyquist curves consist of a semicircular section and a linear section. The semicircular portion corresponds to the charge transfer resistance R_{ct} . The Randles equivalence circuit (Fig. 3 inset) includes the electrolyte resistance (R_s), Warburg impedance (Z_w), charge transfer resistance (R_{ct}) and double layer capacitance (C_{dl}). Fig. 3 shows that the GQDs/GCE has a smaller semicircle diameter, and the impedance of the modified electrode was significantly reduced, indicating that GQDs modified on the surface of GCE could obviously decrease the interfacial electron transfer resistance between solution and electrode. This should be mainly attributed to the excellent electrochemical performance of GQDs, which provides a larger effective

surface and more electron transport channels, thereby improving the conductivity of the electrode surface.

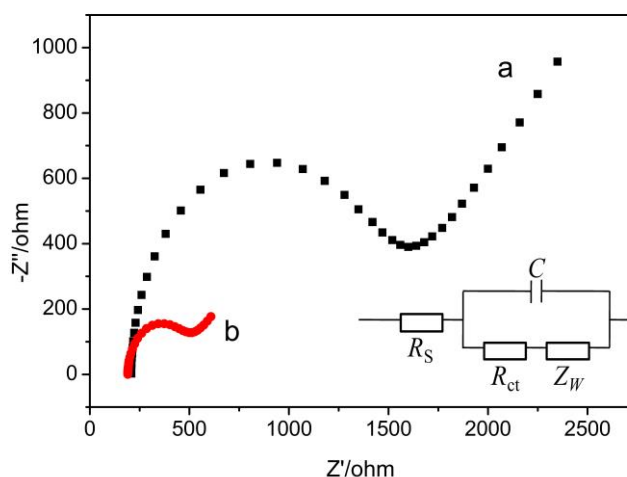


Figure 3. Nyquist plots of different electrodes in 5 mM $[\text{Fe}(\text{CN})_6]^{3-/4-}$ containing 0.1 M KCl [27]: bare GCE (a) and GQDs/GCE (b), inset: the equivalent circuit

3.3 Electrochemical behaviors of HQ and CC on the GQDs/GCE

The electrochemical behaviors of HQ and CC were carefully explored at the GQDs/GCE and bare GCE in 0.1 M PBS (pH 6.5) by CV. Fig. 4A and B shows the CV curves of 0.1 mM HQ and 0.1 mM CC at the different electrodes, respectively. The redox peaks potentials of HQ and CC on GCE (curve b) were 0.283V/-0.070V and 0.359V/0.046V. The potential differences between anodic and cathodic peaks (ΔE_p) were determined to be 353 mV and 313 mV. However, when GQDs was modified on the surface of the electrode, ΔE_p (curve a) of HQ and CC decreased to 40 mV and 38 mV, respectively. Meanwhile, a pair of more apparent redox peak currents of 0.1 mM HQ were detected on GQDs/GCE (Fig. 4A, curve a) compared to than those at bare GCE (Fig. 4A, curve b). Similarly, Fig. 4B revealed that redox peak currents of 0.1 mM CC were larger than those at bare GCE. Fig. 4C shows the CVs recorded for the mixture of HQ and CC at the different electrodes. It can be clearly observed that the redox peaks of HQ and CC were completely unrecognizable on the GCE, whereas two pairs of distinctly well-separated redox peaks were obtained at the GQDs/GCE, the anodic peak potentials (E_{pa}) between HQ (91 mV) and CC (204 mV) were separate with the E_{pa} value of 113 mV, which was larger than that of most literatures [31, 32]. This result suggested that the two phenolic isomers have independent electrochemical response and simultaneous determination on the GQDs/GCE. The superior electrochemical response of HQ and CC on the GQDs/GCE may attribute to high electroactive surface area, good electrocatalytic activity and low charge transfer resistance of GQDs.

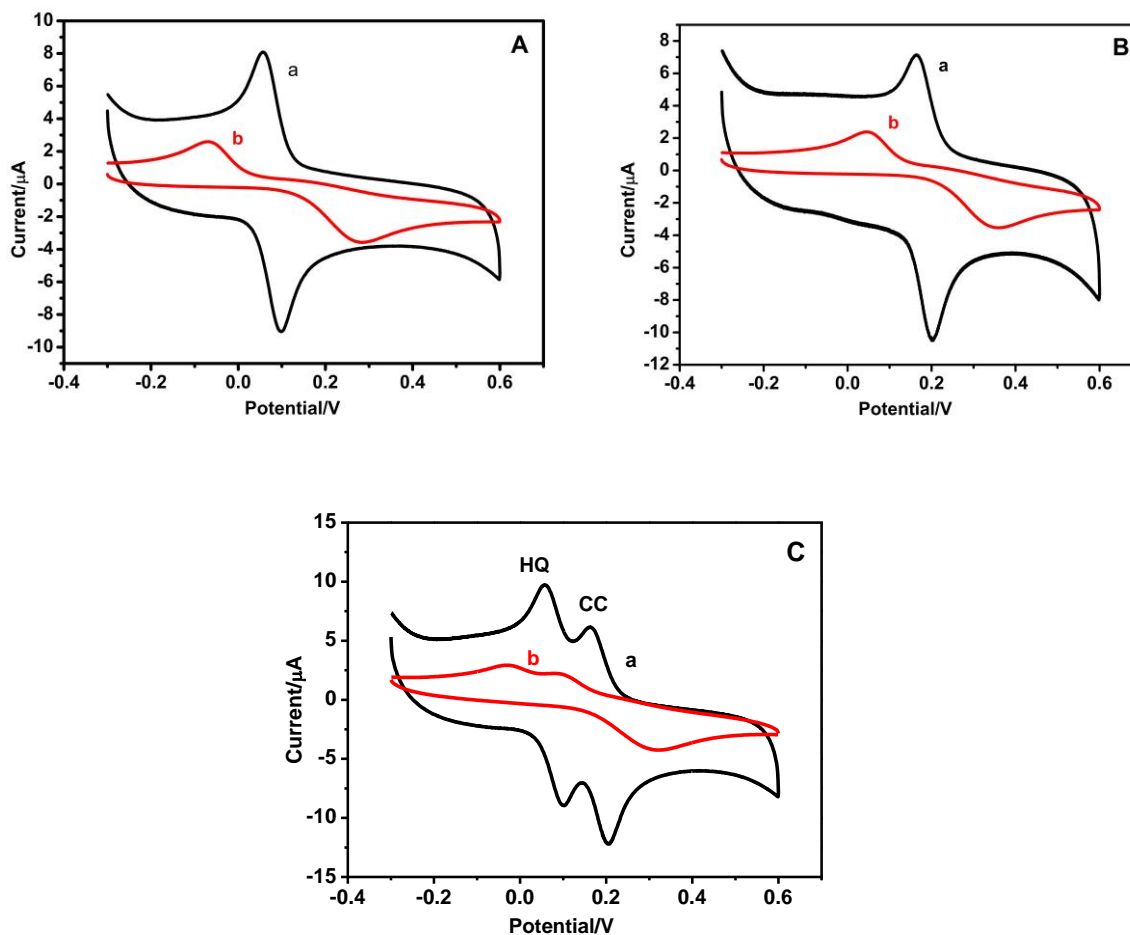


Figure 4. CVs of 0.1 mM HQ (A) , 0.1 mM CC (B) and a mixture solution of 0.1 mM HQ and 0.1 mM CC (C) in 0.1 M PBS (pH 6.5) solution at GQDs/GCE (a) and bare GCE (b)

3.4 Effect of pH value

The influence of pH values (varying from 4.5 to 8.0) on the determination of HQ (0.1 mM) and CC (0.1 mM) in mixed solution was studied on the GQDs/GCE by CV, and the results are shown in Fig. 5. Fig. 5A and 5B exhibited that I_{pa} of HQ and CC slowly increased with increasing pH from 4.5 to 6.5, and then decreased with the increasing of the pH value from 6.5 to 8.0. It may be due to the lack of protons in the solution when the pH was high, which affected the electrochemical reaction. Thus pH 6.5 was chosen as the optimum pH value in order to achieve high sensitivity in subsequent experiment. In addition, Fig. 5B indicates that the relationship between pH and the anodic peak potential. The anodic peak potentials of HQ and CC shifted to more negative with the increase of pH from 4.5 to 8.0. The relations between the peak potential and pH for HQ and CC were expressed as follows:

$$E_{pa} \text{ (mV)} = 0.4699 - 0.0586 \text{ pH} \text{ (R} = 0.997, \text{ HQ)}$$

$$E_{pa} \text{ (mV)} = 0.5109 - 0.0565 \text{ pH} \text{ (R} = 0.997, \text{ CC)}$$

The two regression lines (E_{pa} vs. pH) for HQ and CC were almost parallel, indicating that the peak to peak separation was constant between HQ and CC at different pH [14]. Meanwhile, the slope values of each pH unit (58.6 mV and 56.5 mV) were close to the theoretical value of 59 mV per unit of

pH, suggesting that the electrochemical processes of HQ and CC on the GQDs/GCE have an equal number of electrons and protons transfer, consistent with the previous reports [33, 34]. Facilitation of charge transport of HQ or CC molecules by the GQDs/GCE was schematically shown in Scheme 1:

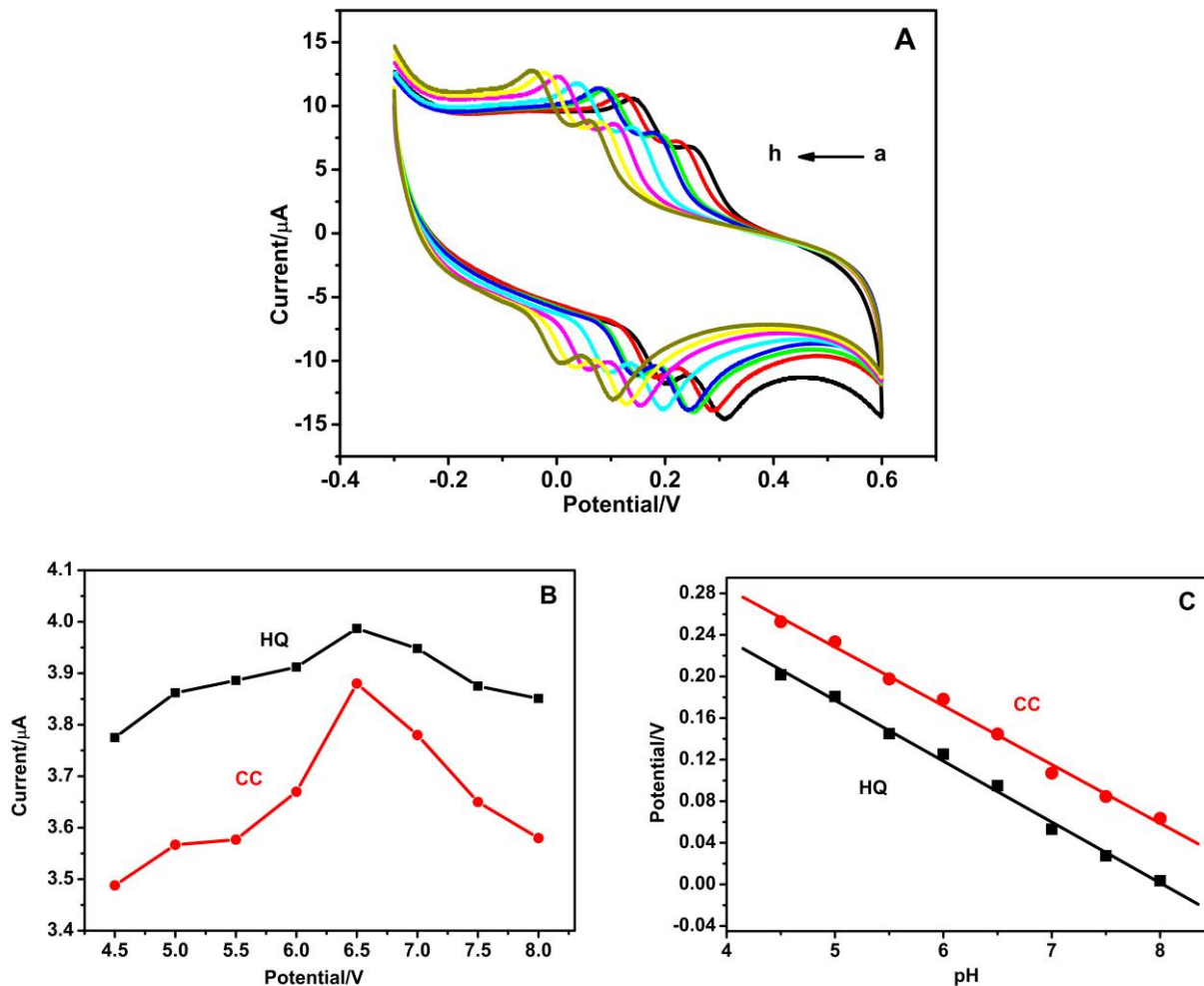
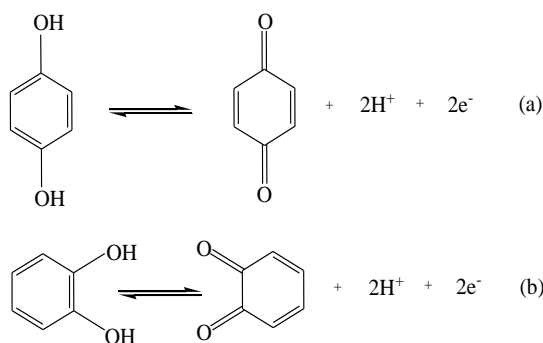


Figure 5. CV of GQDs/GCE in pH 4.5–8.0 PBS containing HQ and CC (A); effect of the pH on the anodic peak currents (B) and anodic peak potentials (C) of HQ and CC (0.1 mM of each).



Scheme 1. the reaction mechanism of HQ (a) and CC (b) on the modified electrode

3.5 Effect of scan rate

The CVs of two hydroxyl benzene isomers at different scan rate of the GQDs/GCE are shown in Fig. 6A. Obviously, the oxidation peak current of the two isomers increased linearly with the square root of the scan rate in the range of 20-200 mV·s⁻¹. As shown in Fig. 6B (curves a and b), the redox peak current as functions of $v^{1/2}$ for the HQ were $I_{pa} = 0.208 v^{1/2} + 0.559$ (μA, mV·s⁻¹, R = 0.996) and $I_{pc} = -0.326 v^{1/2} - 0.332$ (μA, mV·s⁻¹, R = 0.998), respectively. The redox peak current as functions of $v^{1/2}$ for the CC (Fig. 6B, curve c and d) were $I_{pa} = 0.33973 v^{1/2} + 0.3479$ (μA, mV·s⁻¹, R = 0.998) and $I_{pc} = -0.19438 v^{1/2} - 0.8049$ (μA, mV·s⁻¹, R = 0.998), respectively. That indicated that diffusion controlled the redox process of the HQ and CC at this proposed electrode [18, 35].

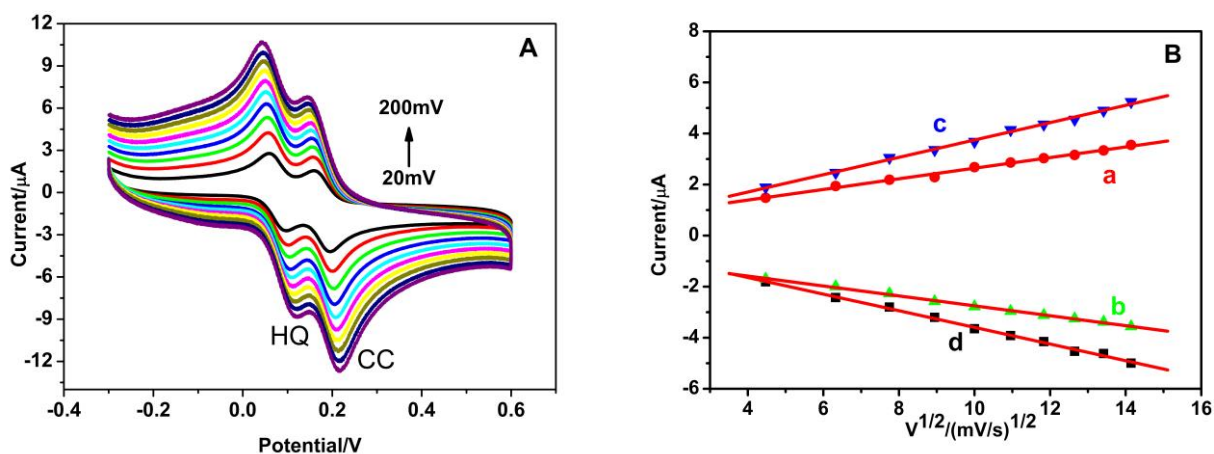


Figure 6. (A) CVs for the mixture solution of HQ and CC (0.1 mM of each) in PBS (pH 6.5) at GQDs/GCE with different scan rates (20, 40, 60, 80, 100,120, 140, 160, 180 and 200 mV·s⁻¹). (B) Plot of peak current density vs. square root of scan rates for HQ and CC (0.1 mM of each).

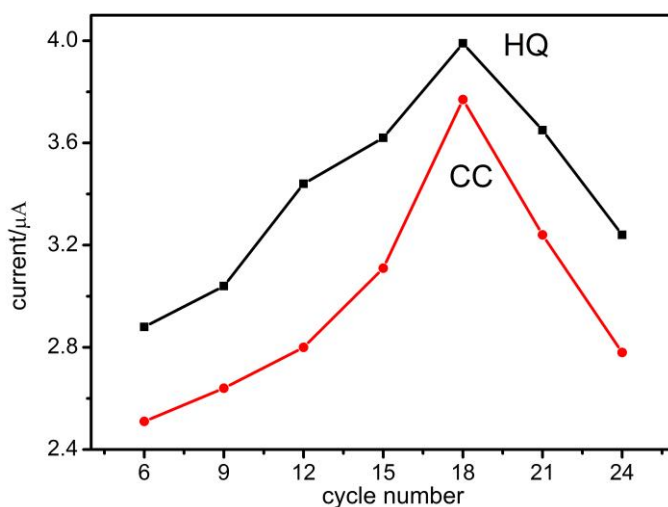


Figure 7. Dependence of the oxidation peak current of CC and HQ on the cycle number during the electrodeposition of GQDs, scan rate: 100 mV·s⁻¹.

3.6 Effect of electrodeposition cycle

It is well known that the thickness of the film is directly related to the number of potential cycles during electrodeposition [36]. The effect of different cycle number of the GQDs in preparation the GQDs/GCE was investigated by the CVs in presence of CC and HQ. Fig. 7 displays the relationship between oxidative peak current and deposition cycle number of GQDs ranging from 5 to 30. Obviously, the oxidative peak current of the two isomers increased with the increasing electrodeposition cycle until the cycle number reached 18. When the cycle of deposition was over 18, the current was slightly decreased. It may be associated with the thickness of GQDs film related to the obstruction of electron transfer on the electrode surface [37]. Thus, cycle number of eighteen was selected as the optimal cycle number in the following experiments.

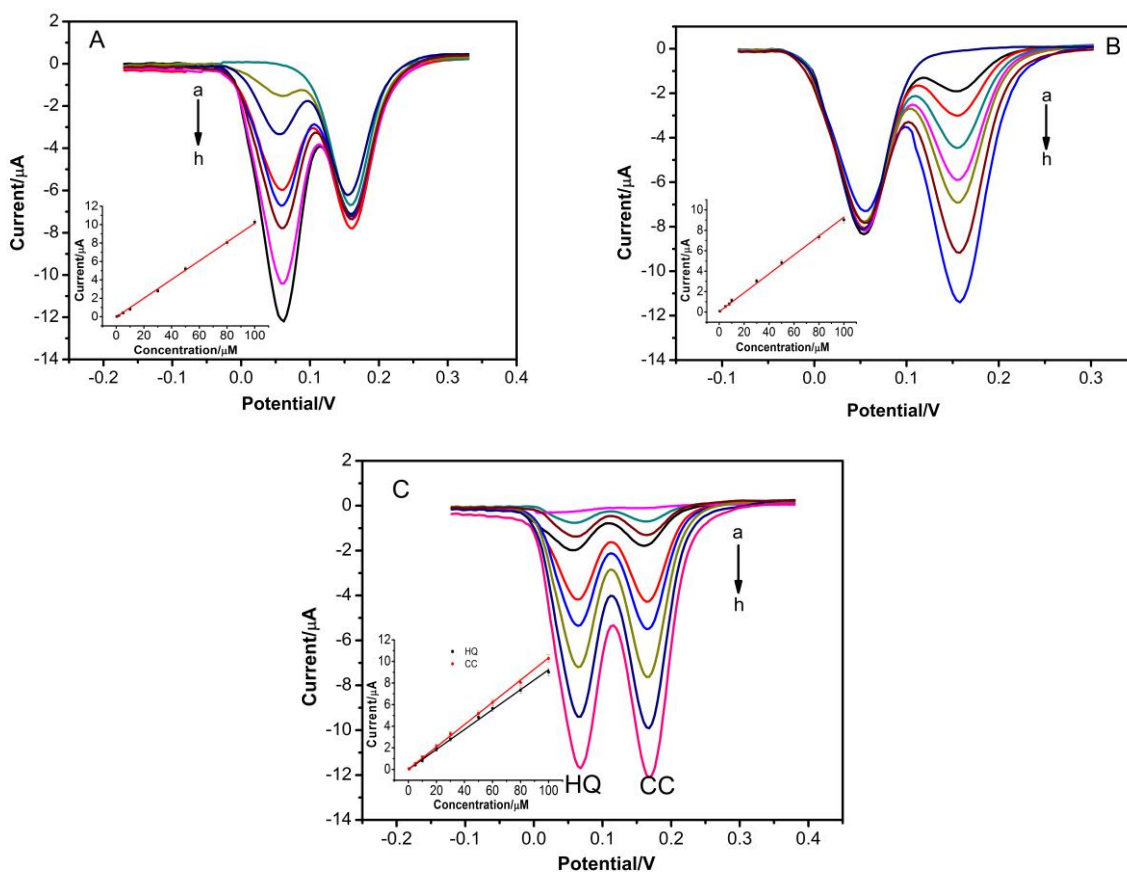


Figure 8. (A) DPVs of GQDs/GCE in the presence of 50 mM CC containing different concentrations of HQ (a to h: 0.5, 2, 5, 10, 30, 50, 80, 100 mM), Inset the dependence of the HQ peak currents on concentrations; (B) DPVs of GQDs/GCE in the presence of 50 mM HQ containing different concentrations of CC (a to h: 0.5, 5, 8, 10, 30, 50, 80, 100 μM), Inset the dependence of the CC peak currents on concentrations.;(C) DPVs of GQDs/GCE in various concentrations of HQ and CC (a to i: 0.5, 5, 10, 20, 30, 50, 60, 80, 100 mM), Inset the relationship of the oxidation peak current with the concentration of HQ and CC.

3.7 Simultaneous determination of HQ and CC

Under the optimal conditions, the simultaneous determination of CC and HQ on the GQDs/GCE was carried out by DPV in 0.1M PBS (pH 6.5). When the concentration of one species changed, the other species was remained constant. Fig. 8A shows the DPV response curves of HQ with different concentrations when the concentration of CC was kept constant (50 μM). From the inset of Fig. 8A, the oxidation peak current of HQ was linear with its concentration in the range of 0.5–100 μM . The regression equation was $I_p (\mu\text{A}) = -0.0322 + 0.1017 C (\mu\text{M}, R = 0.999)$, the detection limit (LOD) for HQ was estimated to be 0.08 μM (S/N = 3). Similarly as shown in Fig. 8B, kept the concentration of HQ constant as 50 μM , the oxidation peak current was proportional to the concentration of CC from 0.5 μM to 100 μM , and the LOD was 0.08 μM (S/N = 3). The regression equation was $I_{pa} (\mu\text{A}) = 0.0351 + 0.0925C (\mu\text{M}, R = 0.997)$.

DPV curves of HQ and CC in the mixture solution by simultaneously changing their concentrations are shown in Fig. 8C. Two well-defined oxidation peaks appeared and the separation of the oxidation peak potentials of HQ and CC was got as 113 mV. The oxidation peak currents (I_{pa}) of HQ and CC increased linearly with their concentrations from 0.5 μM to 100 μM . The regression equations were $I_{pa} (\mu\text{A}) = 0.0034 + 0.0923 C (\mu\text{M}, R = 0.999, \text{HQ})$ and $I_{pa} (\mu\text{A}) = 0.0193 + 0.1032 C (\mu\text{M}, R = 0.999, \text{CC})$, respectively. It can be seen that the presence of isomer did not interfere with the electrochemical detection of another compound, indicating that the GQDs/GCE exhibited good distinguish ability for HQ or CC detection. Compare to the proposed reports (shown in Table 1), this proposed modified electrode for simultaneous detection HQ and CC have a comparable detection limit and acceptable linear dynamic range. Therefore, the GQDs/GCE can also be used for the determination of the dihydroxy benzene isomers either individually or simultaneously.

Table 1. Comparison of analytical performances at different materials-based electrochemical sensors for the simultaneous electrochemical determination of HQ and CC

Materials	Technique	Linear range (μM)		Detection limit (μM)		Reference
		HQ	CC	HQ	CC	
Au-Pd nano-flower/rGO	DPV	1.6-100	2.5-100	0.5	0.8	[36]
(MWNTs/NH ₂ CH ₂ CH ₂ NH ₂)	DPV	10-120	5-80	2.3	1.0	[38]
AuNPs/Fe ₃ O ₄ /APTES/GO	I-T	3-137	2-145	1.1	0.8	[39]
N-GCE	DPV	5-260	5-260	0.2	0.2	[40]
WS ₂ -graphene	DPV	1-100	1-100	0.2	0.1	[41]
NiO/CNT	DPV	10-500	10-400	2.5	2.5	[42]
Gold-graphene	DPV	1-100	1-100	0.2	0.15	[43]
GQDs/GCE	DPV	0.5-100	0.5-100	0.08	0.08	This work

3.7 Reproducibility, stability and selectivity of the GQDs/GCE

Through the use of five independently prepared modified electrodes under the same conditions to explore the reproducibility, the response of a mixed solution of 0.1 mM HQ and 0.1 mM CC was measured. The experiments showed that the relative standard deviation (*RSD*) of HQ and CC were 2.47% and 1.57%, respectively, indicating that the GQDs/GCE had a good reproducibility. Taking into account the electrode stability have an impact on the detection sensitivity, the modified electrode was stored at 4 °C for 2 weeks, the peak current remain 95 % of their initial values. This revealed the good stability and reproducibility of the GQDs/GCE.

The interference of some common ions and other organic compounds was detected in 0.1M PBS (pH 6.5) with 50 μ M HQ and CC. The experimental results showed that 1000 times of K^+ , Ca^{2+} , Na^+ , Al^{3+} , Zn^{2+} , Zr^{2+} , Fe^{2+} , Cu^{2+} , Mg^{2+} , NO_3^- , SO_4^{2-} , CO_3^{2-} and 100 times the dopamine did not interfere with the test (the change of signal was less than 5%). In addition, 5 times phenol, resorcinol and nitrophenol had no obvious effect on the determination, indicating that the GQDs/GCE had high selectivity and anti-interference ability.

3.8 Analytical applications

In order to judge of the practicability of the proposed detection method, the GQDs/GCE was used for simultaneous determination of HQ and CC in the local river (Huai River, Bengbu, China). A mixture of CC and HQ was added to samples of river water, then the amounts of HQ and CC in the real sample were determined by calibration method and the results are shown in Table 2. The recoveries ranged from 97.90 to 102.1% for HQ, and CC ranged from 98.94 to 103.9%. The prepared GQDs/GCE can be available to carry out for the direct simultaneous determination of HQ and CC.

Table 2. Simultaneous determination of HQ and CC in river water samples

Sample	Analyte	Added (μ M)	Found ^a (μ M)	RSD ^b (%)	Recovery (%)
1	HQ	10	9.79 \pm 0.17	1.79	97.90
	CC	90	93.59 \pm 0.21	1.83	103.9
2	HQ	30	30.64 \pm 0.12	2.45	102.1
	CC	70	69.92 \pm 0.17	2.21	99.89
3	HQ	50	49.56 \pm 0.15	1.70	99.12
	CC	50	49.47 \pm 0.19	1.46	98.94
4	HQ	70	70.08 \pm 0.21	1.78	100.1
	CC	30	29.97 \pm 0.11	1.66	99.90
5	HQ	90	90.09 \pm 0.13	1.25	100.1
	CC	10	9.97 \pm 0.14	1.31	99.70

^a Standard addition method. ^b Relative standard deviation for 5 successive measurements.

4. CONCLUSION

In summary, GQDs were synthesized and used as a special sensing material modified on glassy carbon electrode for simultaneous determination of HQ and CC. Due to the excellent electrochemical catalysis and high electroactive surface area of GQDs, the GQDs modified electrode had low detection limits, wide linear range, good repeatability, and good long-term stability. This method was suitable for the direct determination of HQ and CC in river water with satisfactory recovery results. Thus, a sensitive and selective electroanalytical method was developed for the discrimination and measurement of HQ and CC, which hold great potential for electrochemical sensing.

ACKNOWLEDGEMENTS

This work was supported by the Project of Education Department of Anhui Province (KJ2017A506), the key discipline of Anhui Science and Technology University (AKZDXK2015A01), the first discipline of Anhui Science and Technology University and the Student's Platform for Innovation and Entrepreneurship Training Program of China (201710879014, 201710879016, 201810879020).

References

1. J. Wang, J.N. Park, X.Y. Wei and C. W. Lee. *Chem. Commun.*, 9 (2003) 628.
2. J. Yu, W. Du, F. Zhao and B. Zeng, *Electrochim. Acta*, 54 (2009) 984.
3. H.L. Qi and C.X. Zhang, *Electroanal.*, 17 (2005) 832.
4. Y.P. Ding, W.L. Liu, Q.S. Wu and X.G. Wang, *J. Electroanal. Chem.*, 575 (2005) 275.
5. H.S. Yin, Q.M. Zhang, Y.L. Zhou, Q. Ma, T. Liu, L.S. Zhu and S.Y. Ai, *Electrochim. Acta*, 56 (2011) 2748.
6. X. Zhang, S. Duan, X.M. Xu, S. Xu and C.L. Zhou, *Electrochim. Acta*, 56 (2011) 1981.
7. H. Cui, C.X. He and G.W. Zhao, *J. Chromatogr. A.*, 855 (1999) 171.
8. M.F. Pistonesi, M.S. Di Nezio, M.E. Centurión, M.E. Palomeque, A.G. Lista and B.S. F. Band, *Talanta*, 69 (2006) 1265.
9. Y.G. Sun, H. Cui, Y.H. Li and X.Q. Lin, *Talanta*, 53 (2000) 661.
10. S.F. Li, X.Z. Li, J. Xu and X.W. Wei, *Talanta*, 75 (2008) 32.
11. P. Nagaraja, R.A. Vasantha and K.R. Sunitha, *J. Pharm. Biomed.*, 25 (2001) 417.
12. N. Guan, Z. Zeng, Y. Wang, E. Fu and J. Cheng, *Anal. Chim. Acta*, 418 (2000) 145.
13. P.S. Ganesh and B.E. KumaraSwamy. *J. Mol. Liq.*, 220 (2016) 208.
14. J. Du, L.L. Ma, D.L. Shan, Y.R. Fan, L.P. Zhang, L. Wang and X.Q. Lu. *J. Electroanal. Chem.*, 722-723(2014) 38.
15. Y.H. Xiang, L. Li, H. liu, Z. Shi, Y.B. Tan, C.Y. Wu, Y.X. Liu and S.H. Zhang. *Sens. Actuators. B*, 267(2018) 302.
16. J.A. Garcia-Mesa and R. Mateos, *J. Agric. Food Chem.*, 55 (2007) 3863.
17. A. Anil Kumar, B. E. Kumara Swamy, P. S. Ganesh, T. Shobha Rani and G. Venkata Reddy, *J. Electroanal. Chem.*, 799(2017) 505.
18. H.L. Wang, Q.Q. Hu, Y. Meng, Z.E. Jin, Z.L. Fang, Q.R. Fu, W.H. Gao, L. Xu, Y.L. Song and F.S. Lu. *J. Hazard. Mater.*, 353(2018) 151.
19. L.A. Ponomarenko, F. Schedin, M.I. Katsnelson, R. Yang, E.W. Hill, K.S. Novoselov and A.K. Geim, *Science*, 320 (2008) 356.
20. S. Zhu, J. Zhang, C. Qiao, S. Tang, Y. Li, W. Yuan, B. Li, L. Tian, F. Liu and R. Hu, *Chem. Commun.*, 47(2011) 6858.
21. J. Shen, Y. Zhu, X. Yang and C. Li, *Chem. Commun.*, 48(2012) 3686.
22. J. Peng, W. Gao, B.K. Gupta, Z. Liu, R. Romero-Aburto, L. Ge, L. Song, L.B. Alemany, X. Zhan and G. Gao, *Nano lett.*, 12 (2012) 844.
23. H.H. Cheng, Y. Zhao, Y.Q. Fan, X.J. Xie, L.T. Qu and G.Q. Shi. *ACS Nano*, 6(2016) 2237.

24. Y. Li, Y. Hu, Y. Zhao, G.Q. Shi, L.E. Deng, Y.B. Hou and L.T. Qu. *Adv. Mater.*, 23(2011) 776.
25. Y.S. Liu, W.Z. Li, J. Li, H.B. Shen, Y.M. Li and Y. Guo. *RSC Adv.*, 6(2016) 43116.
26. Y. Chen, Y. Li, D.M. Deng, H.B. He, X.X. Yan, Z.X. Wang, C.H. Fan and L.Q. Luo, *Biosens. Bioelectron.*, 102(2018) 301.
27. S.B. Zheng, R. Huang, X.Q. Ma, J. Tang, Z.R. Li, X.C. Wang, J.M. Wei and J.F. Wang, *Int. J. Electrochem. Sci.*, 13 (2018) 5723.
28. G Wang, G Shi, X Chen, R Yao and F Chen, *Microchim. Acta*, 182(2015) 315.
29. Y.Q. Dong, J.W. Shao, C.Q. Chen, H. Li, R.X. Wang, Y.W. Chi, X.M. Lin and G.N. Chen, *Carbon*, 50(2012) 4738.
30. J.Y. Huang, T. Bao, T.X. Hu, W. Wen, X.H. Zhang and S.F. Wang, *Microchim. Acta*, 184(2016) 1.
31. X.B. Li, G.R. Xu, X.Y. Jiang and J.Z. Tao, *J. Electrochem. Soc.*, 161 (2014) H464.
32. Y.J. Yang and W.K. Li, *Full. Science Tech.*, 23 (2015) 410.
33. J. Tang and B.K. Jin. *Anal. Methods*, 7(2015) 9218.
34. Y. Chen, X. Liu, S. Zhang, L. Yang, M. Liu, Y. Zhang and S. Yao, *Electrochim. Acta*, 231 (2017) 677.
35. J.H. He, R. Qiu, W. Li, S.H. Xing, Z.R. Song, Q. Li and S.T. Zhang, *Anal. Methods*, 6 (2014) 6494.
36. P. Kalimuthu and S.A. John, *Electrochem. Commun.*, 11 (2009) 367.
37. A. Ahammad, M.M. Rahman, G.R. Xu, S. Kim and J.J. Lee, *Electrochim. Acta*, 56 (2011) 5266.
38. S. Feng, Y. Zhang, Y. Zhong, Y. Li and S. Li, *J. Electroanal. Chem.*, 733 (2014) 1.
39. S. Erogul, S.Z. Bas, M. Ozmen and S. Yildiz, *Electrochim. Acta*, 186 (2015) 302.
40. Y. Wang, Y. Xiong, J. Qu, J. Qu and S. Li, *Sens. Actuators. B*, 223 (2016) 501.
41. K.J. Huang, L. Wang, Y.J. Liu, T. Gan, Y.M. Liu, L.L. Wang and Y. Fan, *Electrochim. Acta*, 107(2013) 379.
42. L. Zhao, J. Yu, S. Yue, L. Zhang, Z. Wang, P. Guo and Q. Liu, *J. Electroanal. Chem.*, 808 (2018) 245.
43. H. Zhang, X. Bo and L. Guo, *Sens. Actuators. B*, 220 (2015) 919.

© 2018 The Authors. Published by ESG (www.electrochemsci.org). This article is an open access article distributed under the terms and conditions of the Creative Commons Attribution license (<http://creativecommons.org/licenses/by/4.0/>).